Research on UAV access deployment algorithm based on improved virtual force model

Shuchang Zhang[1], Duanpo Wu[1,2*], Lurong Jiang[3], Xinyu Jin[4], and Shuwei Cen[5]
[1] School of Communication Engineering, Hangzhou Dianzi University
Hangzhou, 310018, China
[e-mail: zsc_hdu@163.com, wuduanpo@hdu. edu. cn]
[2] Zhejiang Provincial Key Laboratory of Information Processing, Communication and Networking
Hangzhou, 310027, China
[3] School of Information Science and Technology, Zhejiang Sci-Tech University,
Hangzhou 310018, China
[e-mail: jianglurong@zstu.edu.cn]
[4] Department of Information Science and Electronic Engineering, Zhejiang University
Hangzhou, 310027, China
[e-mail: jinxy@zju. edu. cn]
[5] China Mobile Communications Group Zhejiang Co., Ltd. Hangzhou Branch
Hangzhou, 310006, China
[e-mail: censhuwei@126. com]
*Corresponding author: Duanpo Wu

Received April 4, 2022; revised June 7, 2022; accepted July 14, 2022; published August 31, 2022

Abstract

In this paper, a unmanned aerial vehicle (UAV) access deployment algorithm is proposed, which is based on an improved virtual force model to solve the poor coverage quality of UAVs caused by limited number of UAVs and random mobility of users in the deployment process of UAV base station. First, the UAV-adapted Harris Hawks optimization (U-AHHO) algorithm is proposed to maximize the coverage of users in a given hotspot. Then, a virtual force improvement model based on user perception (UP-VFIM) is constructed to sense the mobile trend of mobile users. Finally, a UAV motion algorithm based on multi-virtual force sharing (U-MVFS) is proposed to improve the ability of UAVs to perceive the moving trend of user equipments (UEs). The UAV independently controls its movement and provides follow-up services for mobile UEs in the hotspot by computing the virtual force it receives over a specific period. Simulation results show that compared with the greedy-grid algorithm with different spacing, the average service rate of UEs of the U-AHHO algorithm is increased by 2.6% to 35.3% on average. Compared with the baseline scheme, using UP-VFIM and U-MVFS algorithms at the same time increases the average of 34.5% to 67.9% and 9.82% to 43.62% under different UE numbers and moving speeds, respectively.

Keywords: UAV deployment, virtual force, Harris Hawks optimization algorithm, user perception

This work was supported by the National College Students' innovation and entrepreneurship training program (202110336030), Ministry of Education-China Mobile Research Fund (MCM20-2017-0107) and the open project of Zhejiang Provincial Key Laboratory of Information Processing, Communication and Networking, Zhejiang, China.

http://doi.org/10.3837/tiis.2022.08.008 **ISSN : 1976-7277**

1. Introduction

With the development of 5G, the need of information transmission rate is rapidly increasing. Meanwhile, huge data traffic services make it difficult for existing terrestrial cellular networks to cope with the surge of hotspot UEs, resulting in overloaded terrestrial base stations (BSs). The mobility and distribution of user equipment (UE) in hotspot areas are uneven, which also brings enormous pressure to UEs in hotspot areas serving terrestrial networks. However, as an air base station, unmanned aerial vehicle (UAV) has acquired much attention because it gives priority to deployment flexibility, low cost, and no terrain constraints.

In recent years, researchers have proposed many algorithms that use UAVs to serve ground UEs, generally with several typical research areas. For example, the optimization of 3D locations with different UE densities [1][2] to reduce its number, the algorithm of UAV to help traditional ground base stations supplement coverage [3][4], overload coverage alleviation, energy efficiency optimization [5][6], backhaul line optimization [7]-[9], UAV mobile path optimization and collision avoidance [10][11], etc. Among all these topics, UAV deployment is an important and basic theme.

Earlier studies mainly focused on the research of single UAV deployments. Al Hourani et al. proposed a mathematical model, aiming to obtain the optimal height of a single UAV to maximize the coverage area [12].

However, with the rapid increasement of UE communication quality requirements and the UE distribution complexity, the assistance effect of a single UAV on ground base stations is not ideal. However, multiple UAVs can form a robust network in the air, to cover and serve a large area of hotspots, and the issue of aerial network deployment in a multi-UAV coordination environment becomes particularly important [13].

As more solutions for UAV network formation and collaborative deployment begin to draw attention. Using a game-theoretic approach to establish a non-cooperative framework, Koulali et al. proposed a method to utilize UAV small cells to improve wireless communication coverage requirements [14]. Zhao et al. proposed a centralized algorithm and a distributed algorithm which are applied to UAV deployment with virtual force so that the UAV can better cover ground UEs after pre-deployment [15]. On this basis, Wang et al. proposed a hybrid algorithm by combining the advantages of the two algorithms, which improves the performance of the algorithm to deploy UAVs [16]. As a typical driving resource, mobility is also essential for UAV networks. Shi et al. proposed a multi-UAV path optimization and resource distribution algorithm based on hierarchical deep reinforcement learning, which enables UAVs to more effectively serve UEs with high-speed movement [17]. In the field of UAV deployment， Kong et al. applied the multi-objective particle swarm algorithm to UAV deployment, which can reduce transmit power and improve energy efficiency compared with test schemes such as the multi-objective whale swarm algorithm [18]. Li et al. proposed a UAV deployment strategy according to artificial bee colony algorithm, which deployed UAV in three-dimensional space and achieved good deployment results [19]. Zhang et al. decreased the required number of UAVs as much as possible and optimized the frequency band, basing on the artificial bee colony algorithm. The superiority of swarm intelligence algorithm in UAV deployment has gradually emerged [20]. Ahmad et al. proposed the clustering algorithm and 3D UAV deployment algorithm that can be iteratively called to achieve multi-UAV deployment in the target area. The results show that this algorithm can effectively serve both outdoor and indoor UEs [21]. Jisang et al. obtained the minimum height of UAV deployment according to the elliptical characteristics generated by the inclined antenna and transformed

the UAV 2D deployment problem into a two-dimensional placement problem without losing optimality. Experimental results show that the algorithm can significantly reduce the service energy consumption of UAVs based on its performance which is close to the 2D exhaustive algorithm [22]. Javad et al. formulated the problem of UAV 3D deployment and antenna orientation as an integer linear programming optimization problem [23].

In this paper, we research on the network coverage problem for mobile UEs. Under the premise of ensuring the communication quality of the UE, the UAV's bearing capacity, and the service scope, a UAV access deployment scheme based on the improved virtual force model is proposed. Our algorithm is composed of three stages. In the first stage, a UAV-adapted Harris Hawks Optimization (U-AHHO) algorithm is designed, that is, by introducing a penalty value, the Harris Hawk algorithm can output a set of better results in the multi-UAV deployment problem. In the second stage, a virtual force improvement model based on user perception (UP-VFIM) is designed, which guides the UAV to track hotspot UEs by introducing a virtual force that senses the UE's movement trend, and provides continuous communication services for hotspot areas. In the third stage, a UAV motion algorithm based on multi-virtual force-sharing (U-MVFS) is designed to reduce the interference between the virtual forces that control the movement of the UAV and improve the sensitivity of UAV to the movement of UEs, which enables UAVs to more effectively serve UEs who move at higher rates. The main contributions are as follows:

1) A pre-deployment algorithm based on U-AHHO is proposed. By setting the penalty value, the algorithm can output a set of reasonable deployment locations. This algorithm enables a limited number of UAVs to serve as many hotspot UEs as possible.

2) The UP-VFIM is designed, which can convert the movement trend of UE, the distance between UE and UAV, and the distance between the UAVs into corresponding virtual forces. This algorithm can guide the movement of UAVs and provide continuous and effective services for UE. With the help of this algorithm, UAVs can track hotspot UEs, independently determine the best service location, and prevent collisions.

3) The U-MVFS algorithm is designed, which can significantly improve the sensitivity of UAVs to UE movement trends, and make UAVs serve the UE moving at higher speeds.

Section 2 presents the UAV deployment system model. Section 3 presents the U-AHHO-based pre-deployment algorithm, UP-VFIM, and U-MVFS algorithm. Section 4 evaluates the performance of this scheme by comparing it with the baseline scheme. Section 5 makes a summary of this paper and future work.

2. System Model

The UAV deployment service model considered can be shown in **Fig. 1**, and its communication objects include UAV, BS and UE. UAVs can move flexibly to any position in the sky. UEs are ground communication terminal equipment, including sensors, mobile phones, etc. In this paper, considering the mobility of the UEs whose location may change over time, all UAVs are set to fly at a fixed optimal altitude and equipped with omnidirectional antennas and all UEs and BSs are on the ground. In terms of frequency band allocation, we assume that BS and UAV work in two mutually orthogonal frequency bands without interference between them. However, all UAVs work in the same frequency band, and the UE which is connected to a UAV will be interfered by all other UAVs regardless of whether there is a connection between them. Similarly, all BSs work in the same frequency band, and the UE which is

connected to a BS will also be interfered by other BSs.

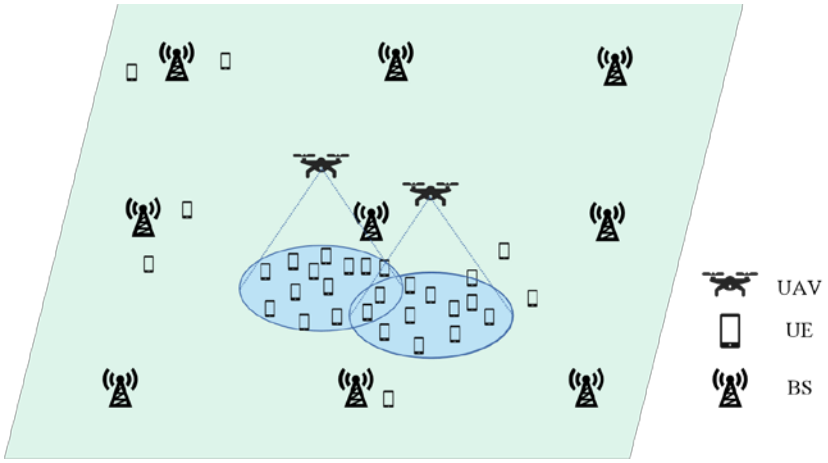

Fig. 1. System model.

2. 1. Channel Model

Let the *i*th UAV, *i*th BS, and *k*th UE be UAV_i, BS_i and UE_k, respectively. For each UAV, in the single link, the UE is directly connected to the UAV, and their transmission channel is an air-to-ground (A2G) channel, whose connection may be blocked by obstacles. Considering the complex terrain of terrestrial terminals, UAV and terrestrial UE channels are usually performed by integrating the probability model of Line-of-sight (LoS) and Non-line-of-sight (NLoS) channels [24].

The LoS link probability between the UAV_i (or BS_i) and the UE_k is:

$$P_{i,k}^{LoS} = \frac{1}{1+\alpha \exp(-\beta(\theta_{i,k}-\alpha))}. \tag{1}$$

where α and β are the related environment modeling parameters, $\theta_{i,k}$ indicates the elevation between the UAV_i and the UE_k, and $\theta_{i,k}$ can be calculated from (2):

$$\theta_{i,k} = \frac{180}{\pi} \times \arctan(\frac{h_u - h_0}{d_{i,k}}). \tag{2}$$

where h_u is the flight height of UAV, h_0 is the height of UE and BS, $d_{i,k}$ is the horizontal distance between UE_k and UAV_i. Consider that the UAVs fly at the same height to the fixed BS, so the elevation $\theta_{i,k}$ between the BS_i and UE_k is equal to 0. The path loss between the UAV_i (or BS_i) and the UE_k can be represented as:

$$g_{i,k}(dB) = P_{i,k}^{LoS} \times L_{i,k}^{LoS} + (1 - P_{i,k}^{LoS}) \times L_{i,k}^{NLoS}. \tag{3}$$

where $L_{i,k}^{LoS}$ and $L_{i,k}^{NLoS}$ are respectively the path loss of the LoS link and NLoS link. They can be obtained by (4) and (5)

$$L_{i,k}^{LoS} = 20\lg R_{i,k} + 20\lg f_0 + 20\lg(\frac{4\pi}{c}) + \eta_{LoS}. \tag{4}$$

$$L_{i,k}^{NLoS} = 20\lg R_{i,k} + 20\lg f_0 + 20\lg(\frac{4\pi}{c}) + \eta_{NLoS}. \tag{5}$$

where η_{LoS} and η_{NLoS} are average extra path loss to the free space propagation loss (FSPL) under LoS and NLoS, respectively. c indicates the speed of light, f_0 is the carrier frequency of the UAV / BS-UE channel. The distance between the UAV_i (or BS_i) and the UE_k are denoted as $R_{i,k}$ which can be obtained by (6):

$$R_{i,k} = \sqrt{h_0^{\ 2} + d_{i,k}^{\ 2}}. \tag{6}$$

Assume that UAV and BS adopt mutually orthogonal frequency bands to serve UEs, the interference between UAV and BS is not considered. If the SINR between UAV_i (or BS_i) and UE_k exceeds a threshold Λ_r, the UE_k can be served. It indicates that the transmission rate and quality of service (QoS) of UE_k can be ensured by the UAV_i (or BS_i). According to [25], the SINR can be calculated by (7):

$$\gamma_{i,k} = \frac{p_{i,k} g_{i,k}}{\sum_{j \neq i} p_{j,k} g_{j,k} + \sigma^2}. \tag{7}$$

where $P_{i,k}$ and $g_{i,k}$ are the transmission power and channel gain of the UAV_i (or BS_i) to the UE_k, respectively. σ^2 indicates the power of the Gaussian white noise. The latter text indicates the transmission power of UAV to UE as p_h, and the transmission power of the BS to UE as p_f.

2. 2 Connection mode

First, let set $M=\{UE_k|k=1, 2, ..., n_e\}$ for all ground UEs, set $F=\{BS_i|i=1, 2, ..., n_b\}$ for all ground BSs, set $U=\{UAV_j|j=1, 2, ..., n_u\}$ for all intended UAVs. The connection status of UE_k and BS_i or UAV_j can be expressed as $\xi_{i,k}^F$ or $\xi_{j,k}^F$. $\xi_{i,k}^F$ is represented as a real matrix with $n_b \times n_e$ dimension, and $\xi_{j,k}^F$ is represented as a real matrix with $n_u \times n_e$ dimension. The matrix elements of the ξ^F and ξ^U are all composed of 0 and 1. Let the maximum UAV perception range be R_s, if the distance between BS_i and UE_k is less than R_s and the value is greater than Λ_r, then $\xi_{i,k}^F$ =1, and otherwise $\xi_{i,k}^F$ =0. Similarly, if the distance between UAV_j and UE_k is less than R_s, and the value is greater than Λ_r, then $\xi_{j,k}^F$ =1, and otherwise $\xi_{j,k}^F$ =0. Therefore, the degrees of BS_i, UAV_j, and UE_k can be expressed as:

$$\rho_i^F = \sum_{k=1}^{n_e} \xi_{i,k}^F. \tag{8}$$

$$\rho_j^U = \sum_{k=1}^{n_e} \xi_{j,k}^U. \tag{9}$$

$$\rho_k^M = \sum_{i=1}^{n_b} \xi_{i,k}^F + \sum_{j=1}^{n_u} \xi_{j,k}^U. \tag{10}$$

Due to the limited resources of BS and UAV, the maximum number of connections for UAV and BS are M_u and M_f respectively, and each UE can just only be connected by one UAV, as same as the BS. Therefore, after the BSs and UEs are connected, redundant connections to them will be removed.

First of all, since this paper studies the UAV-assisted terrestrial network, when the UE meets the connection conditions of several UAVs and BSs at the same time, the UE will preferentially choose to connect with the BS. Secondly, to obtain better communication quality, the UE will choose to connect with the BS with a smaller degree when the UE meets the connection conditions of multiple BSs at the same time. Furthermore, to minimize the input cost of the UAVs to be delivered, when the UE meets the connection conditions of multiple UAVs at the same time, the UE will choose to connect with the UAV with a larger degree and no more than M_u. Finally, when the number of UEs connected with BS or UAV exceeds the respective maximum number of connections, the BS or the UAV will preferentially unload the

UEs with a larger degree value. After the redundant connections are eliminated, we define the service rate of UEs in the area as C, whose calculation method is as follows:

$$C = \sum_{k=1}^{n_e} \rho_k^M . \tag{11}$$

2. 3 Problem formulation

In our proposed model, the main optimization goal is to improve the service rate of UEs in the region. The main optimization objectives of this paper can be expressed as:

$$P: \max \sum_{k=1}^{n_e} \rho_k^M .$$

s. t.

$$C1: \xi^F, \xi^U \in \{0,1\}$$

$$C2: \sum_{i=1}^{n_b} \xi_{i,k}^F + \sum_{j=1}^{n_u} \xi_{j,k}^U \le 1, \forall k$$

$$C3: \sum_{k=1}^{n_b} \xi_{i,k}^F \le M_f, \sum_{k=1}^{n_u} \xi_{j,k}^U \le M_u, \forall j, i$$

$$C4: d_{i,k}, d_{i,k} \le R_s, \forall j, i, k$$

$$C5: \gamma_{i,k}, \gamma_{j,k} \ge \Lambda_r, \forall j, i, k$$

$$C6: n_u \le U_{\max}$$

where $C1$ is a logical constraint for the connection of UAVs and BSs to the UEs. $C2$ represents a UE that only has one connection with all UAVs and BSs. $C3$ indicates that the connection number of UEs to UAVs or BSs cannot exceed the upper limit. $C4$ indicates that the UAVs (or BSs) and the UEs that have a connection relationship will not be able to maintain the connection between them when the distance between them is greater than the sensing range of the UAV. $C5$ indicates that the SINR value between the UE and the UAV (or BS) connections cannot be less than the threshold value of Λ_r. $C6$ indicates that the number of UAVs is in a limited range of $U_{\max}$.

3. UAV deployment and mobile algorithm

3. 1 Basic ideas

To provide continuous and reliable services for UEs in hotspot areas, we should first obtain the coordinates of UEs in hotspot areas. We assume that the position of UE can be obtained by BS or the release of reconnaissance UAVs in advance. The U-AHHO algorithm is then used to achieve the pre-deployment of UAVs in the target area. Next, UP-VFIM is constructed to sense the movement trend of the mobile UE. Finally, the U-MVFS algorithm is applied. At this stage, the UAVs do not need to know the position of the UEs in advance. The UEs within a certain range will be perceived by sensors carried by the UAV. Then the UAVs calculate the virtual forces from different sources and flight to follow the movement of the main population in the hotspot area to provide continuous network assistance to the target area. For clarity, the entire course of the scheme can be shown in **Fig. 2**.

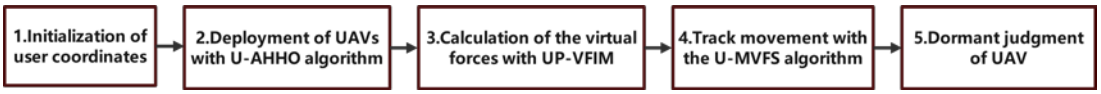

Fig. 2. Flowchart of UAV access deployment algorithm.

3. 2 U-AHHO algorithm

The standard Harris Hawks algorithm is a group intelligent optimization algorithm proposed by Heidari et al. in 2019, which is implemented by mimicking the cooperative and hunting behavior of Harris Hawks populations in nature. Specifically, multiple Harris Hawks will chase the prey in multiple directions to achieve a surprise attack on the prey. Harris Hawks adopt multiple hunting patterns, changing dynamically, depending on their distance from their prey and their prey's escape energy. The proposed algorithm has a strong global search ability. However, for the optimization problem of UAV-assisted ground cellular network, operators often invest more than one UAV, so we introduce the penalty value to propose a U-AHHO algorithm, which can effectively provide a set of superior solutions to the UAV deployment problem. This paper summarizes the symbols used in the algorithm, as shown in **Table 1**. The specific courses of the U-AHHO can be shown in **Fig. 3**:

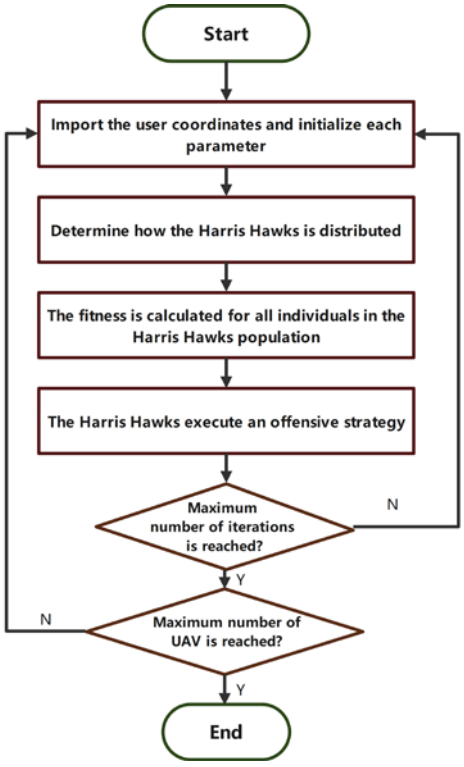

Fig. 3. Basic flowchart of the U-AHHO algorithm

Table 1. Symbols used in the U-HHO algorithm

Symbols	Descriptions
$F=\{BS_i \mid i=1, 2, ..., n_b\}$	Set of BSs
$M=\{UE_k \mid k=1, 2,..., n_e\}$	Set of UEs
$E=\{HH_q \mid q=1, 2, ..., n_h\}$	Set of Harris Hawks
$U=\{UAV_j \mid j=1, 2,..., n_u\}$	Set of UAVs

3. 2. 1 Specific steps of the U-AHHO algorithm

Step 1: Import the UE coordinates to initialize each parameter

Initialize the maximum number of iterations, the Harris Hawks population number, the maximum service range of UAVs, and the maximum number of invested UAVs, which can be denoted as I_{max}, n_h, R_s, *and* n_u, respectively. Assume that the upper and lower limits of the solution space are b_u and b_l, respectively. Let $\boldsymbol{\zeta}$ be the set of contribution degrees of all UEs, and initialize the UE contribution degrees to be 1. $\boldsymbol{\zeta}$ is a $1\times n_e$ dimensional matrix, and each element value in the matrix represents the corresponding contribution degree of UE. $\boldsymbol{\psi}$ represents a matrix with a dimension of $n_e\times n_h$, and the matrix elements are all composed of 0 or 1. If the distance between UE_k and HH_q is less than R_s, the matrix $\boldsymbol{\psi}_{k,p}$=1, and if the distance is greater than R_s, then $\boldsymbol{\psi}_{k,p}$=0.

Step 2: Determine how the Harris Hawks are distributed.

Set X^t is the position of Harris Hawks at time t, X^{t+1} is the position of Harris Hawks at time t+1, X_r^t is a random position within the solution space at time t, X_{prey}^t is the prey position at time t, and X_{ave}^t is the average position of all Harris Hawks at time t. For each iteration, all Harris Hawks undergo location updates through (12):

$$X^{t+1}=\begin{cases} x_r^t - b_1\left|X_r^t - b_2 X^t\right| & e \geq 0.5 \\ (X_{prey}^t - X_{ave}^t) - b_3(b_l + b_4(b_u - b_l)) & e < 0.5 \end{cases}. \tag{12}$$

where e, b_1, b_2, b_3 and b_4 are the random number within [0,1].

Step 3: Calculate the fitness of all individuals in the Harris Hawks population.

The row vector $\mathbf{A}$ indicates the individual Harris Hawks fitness. To facilitate the following representation, we represent the fitness value of HH_q as $\mathbf{A}(q)$, where $\mathbf{A}$ can be matrix calculated by (13), and for each iteration, $\mathbf{A}$ gets an update.

$$\mathbf{A}=\boldsymbol{\zeta}\cdot\boldsymbol{\psi}. \tag{13}$$

Step 4: Set the most fitness Harris Hawks as the prey.

To obtain the optimal deployment position, the position of the Harris Hawks who have the greatest fitness is set to be the position of the prey, and other Harris Hawks develop their surroundings through different strategies to observe whether there is a better deployment point.

Step 5: The Harris Hawks execute four offensive strategies.

Assuming that the P is the escape energy of the prey, which determines whether the Harris Hawks is in the global search or local development phase, the P_0 is a random number between [-1,1]. The escape energy can be calculated by (14):

$$P=2P_0(1-t/I_{\max}). \tag{14}$$

For each iteration, the Harris Hawks perform four different offensive strategies following the prey's escape energy for the distance between them.

When $|P|\geq 1$, let R_{prey} be a random number between [0,1]. The jumping distance during the escape of the prey can be obtained by (15)

$$K=2\times(1-\lambda). \tag{15}$$

where λ is a random number between the [0,1]. The location of the individual Harris Hawks is updated by (12):

Method 1: Soft siege

When the $R_{prey}\geq 0.5$ and $|P|\geq 0.5$, the Harris Hawks location updates can be found by (16):

$$X^{t+1}=X_{prey}^t - X^t - P\left|K\cdot X_r^t - X^t\right|. \tag{16}$$

Method 2: Hard besiege

When $R_{prey} \geq 0.5$ and $|P| < 0.5$, the Harris Hawks location updates can be found by (17):

$$X^{t+1} = X^{t}_{prey} - P\left|X^{t}_{prey} - X^{t}\right|. \tag{17}$$

Method 3: Soft besiege with progressive rapid dives

When $R_{prey} < 0.5$ and $|P| \geq 0.5$, the Harris Hawks location updates can be found by (18):

$$X^{t+1} = \begin{cases} Y & if \quad \mathbf{A}(Y) < \mathbf{A}(X^{t}) \\ Z & if \quad \mathbf{A}(Y) < \mathbf{A}(X^{t}) \end{cases}. \tag{18}$$

where the specific functions of the Y and Z functions are (19) and (20), respectively:

$$Y = X^{t}_{prey} - P\left|K \cdot X^{t}_{prey} - X^{t}\right|. \tag{19}$$

$$Z = Y + S \times LF(D_{IM}). \tag{20}$$

where D_{IM} is the dimension of the deployment algorithm, S is a random vector with $1 \times D_{IM}$ dimension, LF function is the Levy flight function, and the specific expression is (21):

$$LF = 0.01 \times \frac{u \times \delta}{\left|v\right|^{\frac{1}{\beta}}}. \tag{21}$$

where u, v are random values between [0, 1], β is set to be 1.5, δ can be obtained by (22):

$$\delta = \left\{ \frac{\Gamma(1+\beta) \times \sin(\frac{\pi\beta}{2})}{\Gamma(\frac{1+\beta}{2}) \times \beta \times 2^{\frac{\beta-1}{2}}} \right\}^{\frac{1}{\beta}}. \tag{22}$$

Method 4: Hard besiege with progressive rapid dives

When $R_{prey} < 0.5$ and $|P| < 0.5$, the Harris Hawks location updates can be found by (23):

$$X^{t+1} = \begin{cases} Y & if \quad \mathbf{A}(Y) < \mathbf{A}(X^{t}) \\ Z & if \quad \mathbf{A}(Y) < \mathbf{A}(X^{t}) \end{cases}. \tag{23}$$

where the functions of the Y and Z based on the new rule can be calculated by (24) and (27), respectively:

$$Y = X^{t}_{prey} - P\left|K \cdot X^{t}_{prey} - X^{t}_{ave}\right|. \tag{24}$$

$$Z = Y + S \times LF(D_{IM}). \tag{25}$$

Step 6: Output the optimal solution position.

Perform steps 2 to 5 until the maximum number of iterations, and output the position X^{j}_{best} of the optimal solution.

Step 7: Calculate the penalty value and update the UE contribution degrees.

Record the position of the optimal solution, give corresponding penalty values for the contribution of different UEs and perform steps 1 to 6 until the maximum number of UAVs reaches, and then output the position set X_u of the optimal solution.

3. 2. 2 Setting of the penalty value

Multiple UAVs are deployed to serve a large area. But if the algorithm is directly executed multiple times, all solutions will appear in almost the same location. To make UAVs as decentralized as possible, We propose to introduce a penalty value that can reduce the communication interference between UAVs and UEs.

Suppose that d_k represents the distance between UE_k and the optimal solution. The optimal solution obtained by each algorithm is recorded until the number of UAV inputs reaches n_u.

The solution set can be denoted as U= {UAV$_j$ | j=1, 2, ..., n_u}. The penalty value can be flexibly adjusted according to the algorithm needs, and here we give a feasible setting scheme, where the UE contribution degrees matrix is updated via (26):

$$\begin{cases} \xi_k(j+1) = \xi_k(j) - P_1 & d_k < R_{p1} \\ \xi_k(j+1) = \xi_k(j) - P_2 & R_{p1} < d_k < R_{p2} \\ \xi_k(j+1) = \xi_k(j) - P_3 & R_{p2} < d_k < R_s \\ 0 & R_s < d_k \end{cases}. \tag{26}$$

where ξ^{j+1} and ξ^{j} are the UE contribution matrix of (j+1)th and jth cycles, respectively. P_1, P_2, and P_3 are all penalty values, and P_1 is much larger than P_2 and P_3, which effectively ensures that the UAV generation position will not be too dense. Here P_1, P_2, P_3, R_{p1} and R_{p2} are set to 10, 0.5, 0.2, 100 m, 200 m, respectively.

Algorithm 1 The U-AHHO algorithm

Requirement: e, I_{max}, b_u, b_l, S_0, R_s, K, Q, u and X_{prey}

```
t=0.
For j=1:n_u
The location of the population according to (12)
  For t=1:I_max
    The Harris Hawks population calculates fitness values as (13)
    Harris Hawks chose the best individual location as the prey location for X_prey
    For each HH_q do
      Update the escape energy P according to (14)
      If |P |>1
        Update the individual Harris Hawk location according to (12)
      Elseif R_prey≥0. 5 and |P |≥0. 5
        Update the individual Harris Hawk location according to (16)
      Elseif R_prey≥0. 5 and |P |<0. 5
        Update the individual Harris Hawk location according to (17)
      Elseif R_prey <0. 5 and |P |≥0. 5
        Update the individual Harris Hawk location according to (18)
      Elseif R_prey <0. 5 and |P |<0. 5
        Update the individual Harris Hawk location according to (23)
      End if
    End for
  End for
  The best prey location ( X_best^j ) obtained is assigned to X_u (j)
End for
Output X_u
```

3. 3 UP-VFIM

When UAV serves UE in the air, there are three different sources of virtual force. The virtual force $\vec{F}_s$ guides the UAV to track UE. The virtual force $\vec{F}_a$ keeps the position of the UAV in the center of the hotspot as far as possible. Virtual force $\vec{F}_c$ prevents excessive proximity between different UAVs from resource waste caused by the excessive overlap of UAV

coverage and prevents UAV collision.

3. 3. 1 Perceived force

As shown in **Fig. 4,** first, at the initial time t_0, the UAV will perceive all UEs within the range of R_s-ε from itself, and record the numbers of these UEs. Assume that the sensing cycle, the sum number of UEs, and the sum of vectors that are directed from the UAV to these UEs can be denoted as T_c, m_{s1}, and $\mathbf{S_1}$ respectively. Second, not only the number of UEs which are in the sensing range of UAV and recorded in the last cycle will be calculated every sensing cycle, but m_{s1} and $\mathbf{S_1}$ will be updated. Let the number of UEs and the sum of vectors that are directed from itself to these UEs be m_{s2} and $\mathbf{S_2}$, respectively.

Let a_1 be the perceptual force parameter, the perceived force $\vec{F}_s$ of the UAV subject to the UE movement trend direction can be obtained by (27):

$$\vec{F}_s = a_1 \times \frac{\mathbf{S}}{m_{s1}}. \tag{27}$$

where $\mathbf{S}$ is the sum of $\mathbf{S_1}$ and $\mathbf{S_2}$ which is shown in **Fig. 4**.

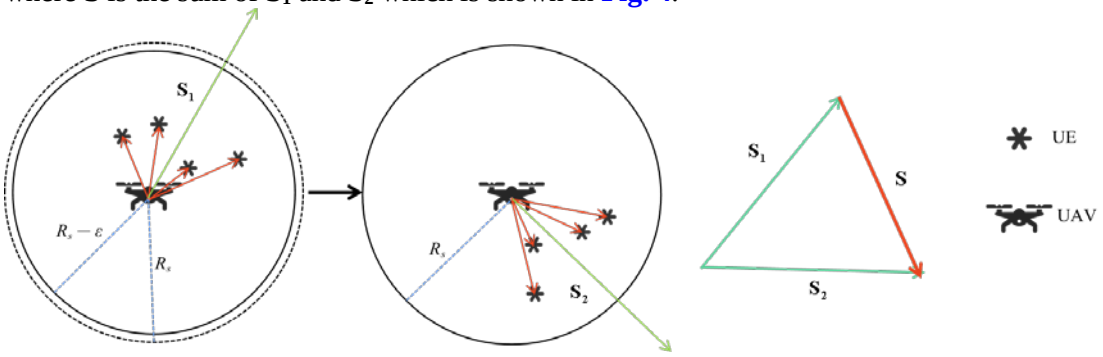

Fig. 4. Schematic representation of the perceived force.

Algorithm 2 The perceived force calculation algorithm

Requirement: T_{max}, T_c and n

1. For each UAV
2. UAV perceives all UEs within the range of R_s-ε
3. UAV records m_{s1}, $\mathbf{S_1}$, and the perceived UE's number
4. End for
5. While $t < T_{max}$
6. For $t = 1+T_c$: T_c: T_{max}
7. For each UAV
8. UAV senses all UEs recorded before T_c within the range of R_s
9. UAV records m_{s2}, $\mathbf{S_2}$ and calculates $\mathbf{S}$
10. UAV calculate the perceived force according to (27)
11. End for
12. For each UAV
13. UAV perceives all UEs within the range of R_s-ε
14. UAV records m_{s1}, $\mathbf{S_1}$, and the perceived UE's number
15. End for
16. End for
17. End while

3. 3. 2 Attractive force

As shown in **Fig. 5**, The UAV perceives all UEs within the range of R_s from itself, and the number of UEs is recorded as m_{s2}, the sum of vectors that are directed from the UAV to these UEs can be denoted as $\mathbf{S_3}$. The attractive forces of UAV by UE_i can be obtained through (28):

$$\vec{F}_a^i = a_2 \times \frac{\mathbf{S_3}}{m_{s2}} \tag{28}$$

where a_2 is the attractive forces parameter.

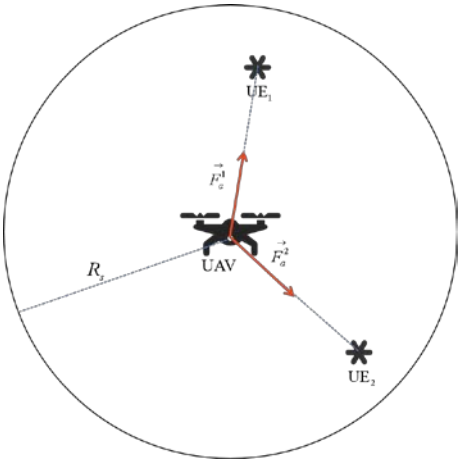

Fig. 5. Schematic representation of the attraction forces

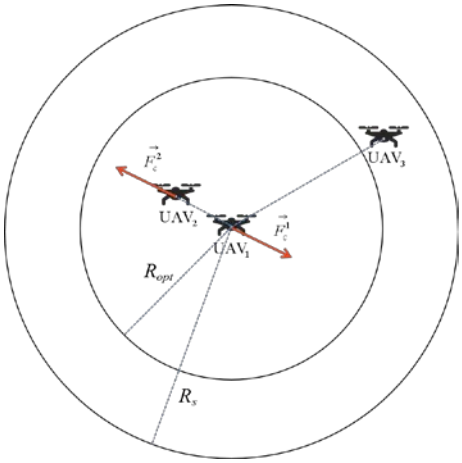

Fig. 6. Schematic representation of the repulsive force.

3. 3. 3 The repulsive force

As shown in **Fig. 6**, the R_{opt} is assumed to be a safe distance between the two UAVs. a_3 is the repulsion parameter, and the UAV senses itself with all the UAVs within the range of R_s. For a UAV with a spacing less than R_s, assuming the UAV direction vector $\mathbf{d}$, the UAV_i pulsion $\vec{F}_c^j$ can be computed by (29):

$$\vec{F}_c^j = \begin{cases} a_3\left(1-\dfrac{R_{opt}}{|\mathbf{d}|}\right)\cdot\dfrac{\mathbf{d}}{|\mathbf{d}|} & (|\mathbf{d}| < R_{opt}) \\ 0 & (R_{opt} \le |\mathbf{d}|) \end{cases}. \tag{29}$$

3. 3. 4 Transformation of virtual force to speed

Since the speed of UAV is limited, we map the virtual force received by the UAV to a speed value according to the method of [16], assuming that the maximum value of the speed of UAV is V_{max}, the virtual force received by the UAV at a certain time is $\vec{F}$, then the flight speed of the UAV $\mathbf{v}$ can be obtained by formula (30):

$$\mathbf{v} = \arctan\left(\left|\vec{F}\right|\right) \times \frac{2}{\pi} \times V_{\max} \times \frac{\vec{F}}{\left|\vec{F}\right|}. \tag{30}$$

3. 4 U-MVFS algorithm

Considering that the repulsive force to ensure the distance between UAVs must be large, and the UAV is extremely sensitive to the movement trend of UE, which will be greatly reduced by the traditional virtual force combined with the resultant force.

3. 4. 1 Multi-virtual force time-sharing

To deal with the above situation, the idea of multi-virtual force time-sharing is proposed. As shown in **Fig. 7**, the maximum service duration of the UAV and the duration of each motion cycle are set to be T_{max} and T, respectively. Then, each motion cycle is equally divided into n segments on average, and the time interval allocation of all UAVs is kept synchronized. The first time segment of each motion cycle is assigned to perceived force which is calculated by the UAV. The second and the third segments are assigned to the repulsive force and attractive force, respectively. For the remaining unallocated segments, the UAV will not calculate the virtual force, and will only be relatively stationary with the ground to provide services for UEs.

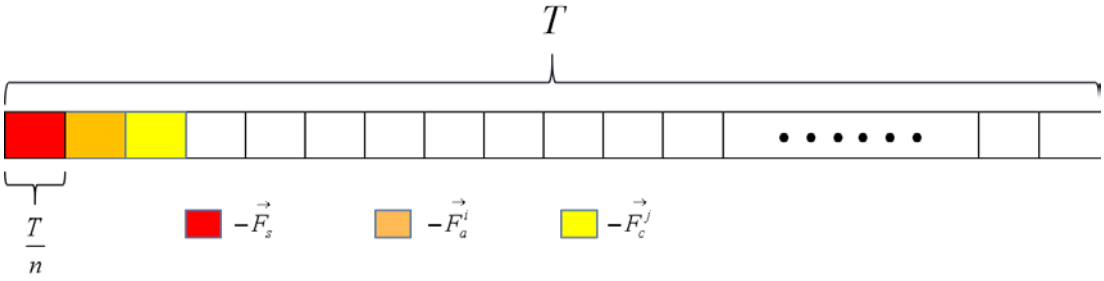

Fig. 7. Schematic diagram of the time interval division.

The application of the multi-virtual force time-sharing UAV motion algorithm aims to reduce the impact of repulsion on perception. In the case that the ability of the UAV to sense the trend of the UE is improved, the energy consumption of UAV movement can be reduced by enlarging T and n to some extent.

Algorithm 3 UAV motion algorithm based on U-MVFS

Requirement: T_{max}, T and T_n

```
For t1=1:Tmax/T
    For t2=1:Tn
        If UAV in the perceptual force corresponding to the time interval do
            Calculate the perceived force of UAV according to(27)
            Calculate the UAV speed and update the position according to (30)
        Elseif UAV in the attraction corresponds to the time interval do
            Calculate the attractive force of UAV attractive forces according to (28)
            Calculate the UAV speed and update the position according to (30)
        Elseif UAV is in the corresponding time interval do
            Calculate the repulsive force of UAV according to (29)
            Calculate the UAV speed and update the position according to (30)
        Else
            The UAV remains stationary and suspended
        End if
    End for
End for
```

3. 4. 2 Dormant judgment of UAV

In the process of serving the UEs, the UAV will try to offload all the connected UEs to the ground BS. If the UEs is successfully uninstalled, the UAV will enter the dormant state, and the dormant UAV will return to the UAV center. Otherwise, the UEs cannot be uninstalled completely and the UAV will continue to work.

4. Results and analysis

In this section, we consider that the UEs are distributed in a 4000 m×4000 m region, and the walking speed of the UE is V_p. The algorithm is used the MATLAB tool to analyze the performance. We consider different deployment scenarios, and the simulation parameters are shown in **Table 2**.

Table 2. Simulation parameters

Parameters	Value
α	9. 6
β	0. 28
f_0	2 GHz
η_{LoS}	1 dB
η_{NLos}	20 dB
σ^2	-140 dBm
Λ_r	-5 dB
R_s	500 m
R_{opt}	230 m
M_u	40
M_f	40
p^h	43 dBm
p^f	46 dBm
I_{max}	200
ε	10 m
T_{max}	2000 s
a_1	2
a_2	0. 2
a_3	1000
V_{max}	10 m/s
h_u	100 m
h_0	0 m
v_p	1 m/s
T	10 s
n	10

The main evaluation index for the performance of the UAV access deployment algorithm is the service rate of UEs in the area. To have an assurance of the accuracy of the conclusion, the following results are obtained by taking the average value of multiple simulations.

First, the deployment performance of the U-AHHO algorithm is studied. In this paper, three hotspot clusters with different radius and different number of people are generated in the target area. The total number of people in the area and the number of available UAVs is set to be 400 and 10, respectively. With the deployment of the U-AHHO algorithm, the deployment location can be shown in **Fig. 8**.

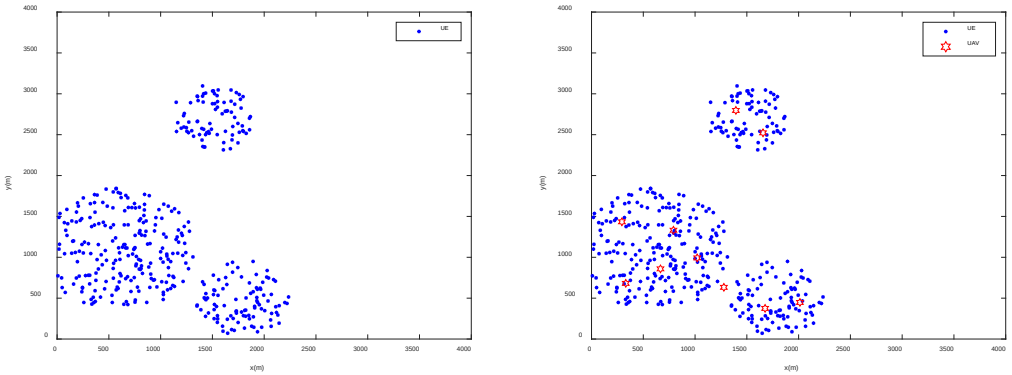

(a) (b)

Fig. 8. The UE distribution map. (a)before deployment of the U-AHHO algorithm. (b)after deployment of the U-AHHO algorithm.

Fig. 8 shows that after the target area is deployed with the U-AHHO algorithm, In **Fig. 8** (b), UAVs are uniformly and reasonably deployed in hotspots. More UAVs are deployed in hot spots with larger UEs clusters, fewer UAVs are deployed in hot spots with smaller UEs clusters and UAVs will not be deployed in areas without UEs. To further reflect the superiority of U-AHHO algorithm, we compare it with the greedy-grid algorithm, in which the grid points at different distance intervals will be calculated and a group of grid points covering a larger number of UEs will be selected as the UAV deployment point. The comparison index is the service rate of UEs. The result is shown in **Fig. 9**.

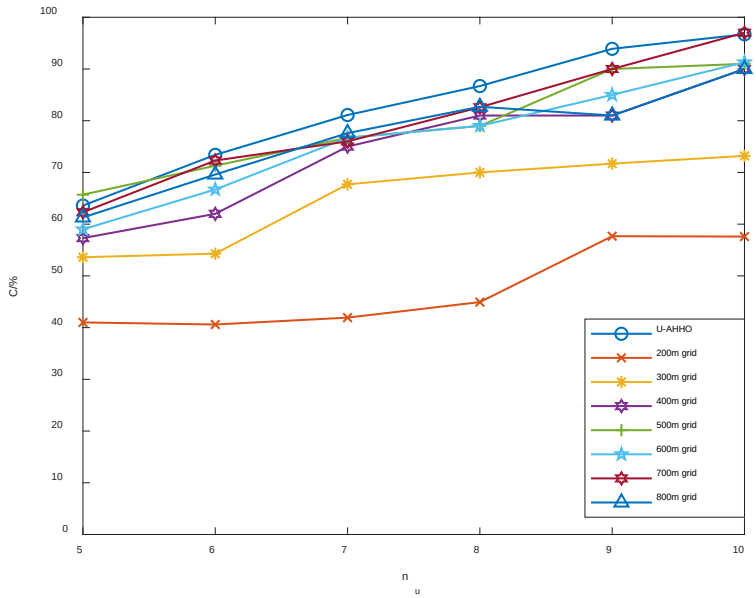

Fig. 9. service rate of UEs with different deployment algorithms.

As can be seen from **Fig. 9**, when there are 400 UEs in the hotspot, and the number of input UAVs is variable. Compared with the greedy-grid algorithm of 200 m, 300 m, 400 m, 500 m, 600 m, 700 m and 800 m, the effect of the U-AHHO algorithm is more stable. A higher service rate of UEs can be maintained when the number of UAVs varies. The deployment with the

greedy-grid algorithm is more random. When the grid points happen to be in a dense area of UEs, it will bring a higher service rate of UEs. For example, the UE service rate of the 500 m greedy-grid algorithm when 5 UAVs are deployed in **Fig. 9** is better than the U-AHHO algorithm, but the overall effect of the 500 m greedy-grid algorithm is inferior to the U-AHHO algorithm and the 700 m greedy-grid algorithm. However, to reflect the overall effect of the scheme more clearly, this paper uses the average service rate of UEs as the indicator. The result is shown in **Fig. 10**.

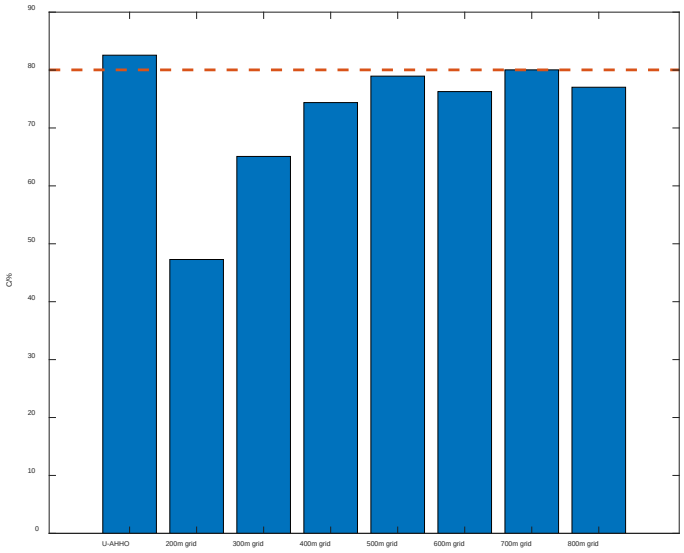

Fig. 10. Average service rate of UE with different deployment algorithms.

From **Fig. 10**, compared with the greedy-grid algorithm of 200 m, 300 m, 400 m, 500 m, 600 m, 700 m, and 800 m, the average service rate of UEs with the U-AHHO algorithm increases by 35.3%, 17.5%, 8.2%, 3.7%, 6.3%, 2.6%, and 5.6%, respectively. More importantly, compared with the greedy-grid algorithm, which is greatly affected by grid spacing, and UE distribution, the U-AHHO algorithm has strong adaptability to various UE distributions, making it more suitable for solving practical problems in complex UE distribution states in scenarios.

To explore the service effect of the UP-VFIM and U-MVFS algorithms on UEs in hotspot areas, we consider the case that different numbers of UEs from three hotspots form a larger hotspot. The distribution of ground base stations is shown in **Fig. 11**. In the process of hotspot moving, the average service rate of UEs in the target area varies with the number of UEs under different algorithm applications as shown in **Fig. 12**. The following results are all pre-deployed with the U-AHHO algorithm.

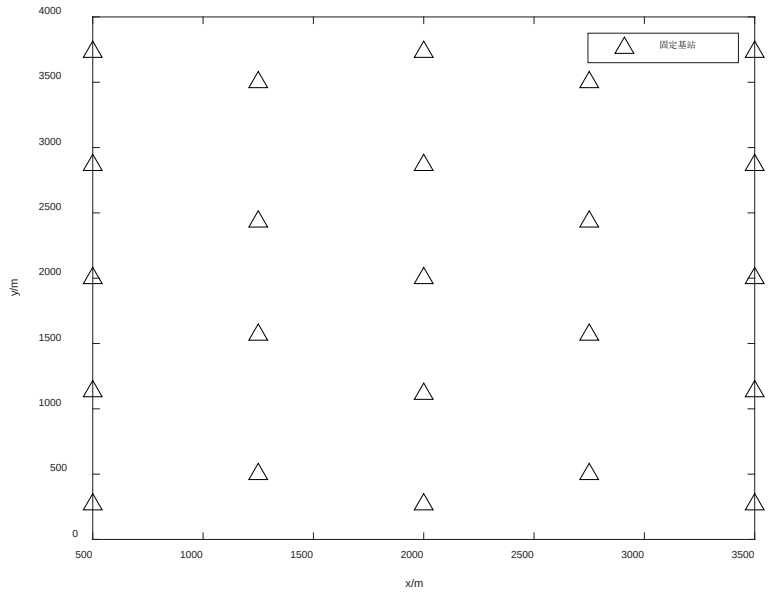

Fig. 11. Distribution diagram of the ground base stations in the target area.

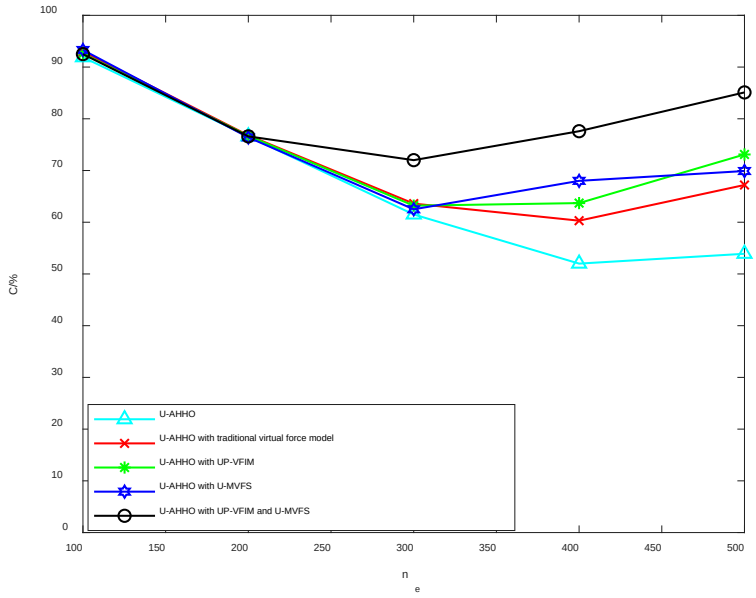

Fig. 12. Average service rate of UEs with different numbers of UEs (v_p=2m/s).

Fig. 12 simulates the improvement effect of various algorithms in the average UE service rate during UE movement in the target area under different numbers of UEs. The result shows that, when the number of UEs is 100, the ground base station can well serve UEs in hotspot areas, so the effect of various algorithms is no different. As the number of UEs increases, the ground base stations are gradually overloaded. At this time, UAVs begin to play a role in relieving the pressure on the ground network. As shown in **Fig. 12**, compared with other algorithms, U-AHHO with UP-VFIM and U-MVFS algorithm are more effective in improving

the overload situation of ground base stations. Compared with U-AHHO, U-AHHO with traditional virtual force model, U-AHHO with U-MVFS, and U-AHHO with UP-VFIM has an average improvement of 67. 9%, 42. 6%, 33. 7% and 34. 5%, respectively. As shown in **Fig. 12**, the inflection point appears when the number of UEs reaches 300 in the scheme using the UP-VFIM algorithm, indicating that if the number of UEs reaches a high level, UAV can use UP-VFIM to sense the movement trend of the UE and effectively follow the hotspot movement. In this way, the pressure on the ground network in the region is relieved to a great extent. The improvement trend of using UP-VFIM and U-MVFS algorithm at the same time is more obvious, which means that with the help of the U-MVFS algorithm, UAV can be more sensitive to the moving trend of UE.

To better explore the performance of the U-MVFS algorithm, without considering the ground base station, it is assumed that 500 UEs from three hotspots form a larger hotspot. Taking the speed of UEs as a variable, the sensitivities of different algorithms to UE movement are explored, as shown in **Fig. 13**.

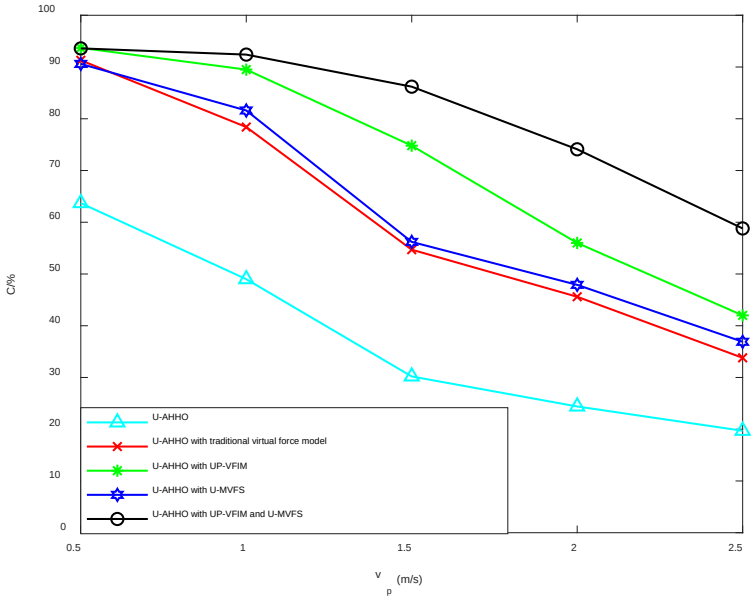

Fig. 13. Average service rate of UEs with different speeds of UEs. (The number of UEs is 500).

In **Fig. 13**, when the UE in the target area moves at a higher speed, the average UE service rate for the target area is reduced by different algorithms. However, using UP-VFIM and U-MVFS algorithm at the same time decreases the average service rate of UEs more slowly than other algorithms. This shows that the simultaneous use of UP-VFIM and U-MVFS algorithms enables UAVs to follow effectively when facing UEs moving at higher speeds. U-AHHO with UP-VFIM and U-MVFS algorithm compared with U-AHHO, U-AHHO with traditional virtual force model, U-AHHO with U-MVFS, and U-AHHO with UP-VFIM improved in average by 43.62%, 20.26%, 9.82%, and 14.38%, respectively.

In addition, the effect of using UP-VFIM and U-MVFS algorithm at the same time is better than only using UP-VFIM, and the effect of using only UP-VFIM is better than using only the U-MVFS algorithm. It is verified that U-MVFS is based on UP-VFIM. UAV can perceive the moving trend of UEs, while U-MVFS further improves the ability of UAV to perceive the moving trend of UEs. The reason why only U-MVFS is slightly better than traditional virtual

force is that U-MVFS only improves the anti-interference ability of the attractive force of UEs to UAV in traditional virtual force, but the attractive force of UEs to UAV contributes to the tracking movement of UAVs which is much smaller than the perception in UP-VFIM, so the effect is minimal.

5. Conclusion and Future Work

This paper proposes a solution to deploy multiple UAVs to assist the ground network to serve UEs and optimizes the deployment and mobility of UAVs to reduce the amount of required UAVs. The contributions of this paper are mainly divided into three parts: 1) Pre-deploy UAVs in hotspot areas by applying the U-AHHO algorithm. 2) Establish the model of UP-VFIM to ensure that UAV can follow hotspot UE and prevent the collision. 3) Propose the algorithm of U-MVFS, to ensure that the UAV can follow the hotspot UE more effectively. Simulation results shows the average service rate of UEs of the U-AHHO algorithm is increased by 2.6% to 35.3% on average, comparing with the greedy-grid algorithm with different spacing. Comparing with the baseline scheme, applying the UP-VFIM and U-MVFS algorithms at the same time increases the average of 34.5% to 67.9% and 9.82% to 43.62% under different UE numbers and moving speeds, respectively.

In the network considered in this algorithm, UAVs are at the same height, but in practical application scenarios, the flying height of UAVs has a certain relationship with the coverage area, which will further increase the complexity of the algorithm. Therefore, further research can be carried out on the UAV deployment and tracking motion algorithms in 3D space.

References

[1] Huang H, Savkin A V, "Deployment of Heterogeneous UAV Base Stations for Optimal Quality of Coverage," *IEEE Internet of Things Journal*, 2022. Article(CrossRef Link)

[2] Nasr-Azadani M, Abouei J, Plataniotis K N, "Single-and Multi-Agent Actor-Critic for Initial UAV's Deployment and 3D Trajectory Design," *IEEE Internet of Things Journal*, 2022. Article(CrossRef Link)

[3] Wu H, Tao X, Zhang N, et al, "Cooperative UAV cluster-assisted terrestrial cellular networks for ubiquitous coverage," *IEEE Journal on Selected Areas in Communications*, vol. 36, no. 9, pp. 2045-2058, 2018. Article(CrossRef Link)

[4] Lyu J, Zeng Y, Zhang R, "UAV-aided offloading for cellular hotspot," *IEEE Transactions on Wireless Communications*, vol. 17, no. 6, pp. 3988-4001, 2018. Article(CrossRef Link)

[5] Thammawichai M, Baliyarasimhuni S P, Kerrigan E C, et al, "Optimizing communication and computation for multi-UAV information gathering applications," *IEEE Transactions on Aerospace and Electronic Systems*, vol.54, no. 2, pp.601-615, 2018. Article(CrossRef Link)

[6] Shakoor S, Kaleem Z, Baig M I, et al, "Role of UAVs in public safety communications: Energy efficiency perspective," *IEEE Access*, vol. 7, pp.140665-140679, 2019. Article(CrossRef Link)

[7] Li P, Xu J, "Placement optimization for UAV-enabled wireless networks with multi-hop backhauls," *Journal of Communications and Information Networks*, vol. 3, no.4 pp.64-73, 2018. Article(CrossRef Link)

[8] Zhang S, Ansari N, "3D drone base station placement and resource allocation with FSO-based backhaul in hotspots," *IEEE Transactions on Vehicular Technology*, vol.69, no.3, pp.3322-3329, 2020. Article(CrossRef Link)

[9] Xing N, Zong Q, Tian B, et al, "Nash network formation among unmanned aerial vehicles," *Wireless Networks*, vol. 26, no.26, pp.1781-1793, 2020. Article(CrossRef Link)

[10] Qin Z, Zhang X, Zhang X, et al, "The UAV Trajectory Optimization for Data Collection from Time-Constrained IoT Devices: A Hierarchical Deep Q-Network Approach," *Applied Sciences*, vol. 12, no.5, p.2546, 2022. Article(CrossRef Link)
[11] Hsu Y H, Gau R H, "Reinforcement learning-based collision avoidance and optimal trajectory planning in UAV communication networks," *IEEE Transactions on Mobile Computing*, vol. 21, no.1, pp.306-320, 2022. Article(CrossRef Link)
[12] Al-Hourani A, Kandeepan S, Lardner S, "Optimal LAP altitude for maximum coverage," *IEEE Wireless Communications Letters*, vol. 3, no.6, pp.569-572, 2014. Article(CrossRef Link)
[13] Akpakwu G A, Silva B J, Hancke G P, et al, "A survey on 5G networks for the Internet of Things: Communication technologies and challenges," *IEEE access*, vol. 6, pp. 3619-3647, 2017. Article(CrossRef Link)
[14] Koulali S, Sabir E, Taleb T, et al, "A green strategic activity scheduling for UAV networks: A sub-modular game perspective," *IEEE Communications Magazine*, vol. 54, no.5, pp.58-64, 2016. Article(CrossRef Link)
[15] Zhao H, Wang H, Wu W, et al, "Deployment algorithms for UAV airborne networks toward on-demand coverage," *IEEE Journal on Selected Areas in Communications*, vol.36, no.9, pp.2015-2031, 2018. Article(CrossRef Link)
[16] Wang H, Zhao H, Wu W, et al, "Deployment algorithms of flying base stations: 5G and beyond with UAVs," *IEEE Internet of Things Journal*, vol. 6, no.6, pp.10009-10027, 2019. Article(CrossRef Link)
[17] Shi W, Li J, Wu H, et al, "Drone-cell trajectory planning and resource allocation for highly mobile networks: A hierarchical DRL approach," *IEEE Internet of Things Journal*, vol. 8, on.12, pp.9800-9813, 2021. Article(CrossRef Link)
[18] Kong Z, Wu D, Jin X, et al, "Improved AP Deployment Optimization Scheme Based on Multi-objective Particle Swarm Optimization Algorithm," *KSII Transactions on Internet & Information Systems*, vol. 15, no.4, pp.1568-1589, 2021. Article(CrossRef Link)
[19] Li J, Lu D, Zhang G, et al, "Post-disaster unmanned aerial vehicle base station deployment method based on artificial bee colony algorithm," *IEEE Access*, vol. 7, pp.168327-168336, 2019. Article(CrossRef Link)
[20] Zhang C, Zhang L, Zhu L, et al, "3D Deployment of Multiple UAV-Mounted Base Stations for UAV Communications," *IEEE Transactions on Communications*, vol. 69, no.4, pp.2473-2488, 2021. Article(CrossRef Link)
[21] Sawalmeh A, Othman N S, Liu G, et al, "Power-Efficient Wireless Coverage Using Minimum Number of UAVs," *Sensors*, vol. 22, no.1, p.223, 2022. Article(CrossRef Link)
[22] Alzenad M, El-Keyi A, Lagum F, et al, "3-D placement of an unmanned aerial vehicle base station (UAV-BS) for energy-efficient maximal coverage," *IEEE Wireless Communications Letters*, vol.6, no.4, pp.434-437, 2017. Article(CrossRef Link)
[23] Sabzehali J, Shah V K, Dhillon H S, et al, "3d placement and orientation of mmwave-based uavs for guaranteed los coverage," *IEEE Wireless Communications Letters*, vol.10, no.8, pp.1662-1666, 2021. Article(CrossRef Link)
[24] Mozaffari M, Saad W, Bennis M, et al, "Drone small cells in the clouds: Design, deployment and performance analysis," in *Proc. of 2015 IEEE global communications conference (GLOBECOM). IEEE*, pp.1-6, 2015. Article(CrossRef Link)
[25] Zhou L, Sheng Z, Wei L, et al, "Green cell planning and deployment for small cell networks in smart cities," *Ad Hoc Networks*, vol. 43, pp. 30-42, 2016. Article(CrossRef Link)

Shuchang Zhang is a student of Hangzhou Dianzi University, Hangzhou, China. His main research direction is wireless network communication.

Duanpo Wu received the B.S. degree from the College of Electronics and Information, Hangzhou Dianzi University, in 2009, and the Ph.D. degree from the College of Information Science and Electronic Engineering, Zhejiang University, China, in 2014. Since 2022, he has been an associate professor with Hangzhou Dianzi University, China. His research interests include wireless communication and intelligent signal processing.

Lurong Jiang received the B.S. degree in electronic communication engineering from Zhejiang University in 2004, the M.S. degree in control theory and control engineering from Hangzhou Dianzi University in 2009, and the Ph.D. degree in Circuits and Systems from Zhejiang University in 2015. From 2021 to present, he is an associate professor in School of Information Science and Technology, Zhejiang Sci-Tech University, Hangzhou, China. His research interest includes the signal processing, network science, wireless sensor networks.

Xinyu Jin is a professor in the faculty of Information Science and Electrical Engineering since 1999, Zhejiang University, China. His research interests include network communication and intelligent electronic systems.

Shuwei Cen is currently the network planning supervisor of Hangzhou Branch of China Mobile Communications Group Zhejiang Co., Ltd. He is mainly responsible for network planning and network specification.